American Mineralogist, Volume 74, pages 256–262, 1989

Akrochordite, $(Mn,Mg)_5(OH)_4(H_2O)_4(AsO_4)_2$: A sheet structure with amphibole walls

Paul Brian Moore
Department of the Geophysical Sciences, The University of Chicago, Chicago, Illinois 60637, U.S.A.
Pradip K. Sen Gupta
Department of Geology, Memphis State University, Memphis, Tennessee 38152, U.S.A.
Elmer O. Schlemper
Department of Chemistry, University of Missouri, Columbia, Missouri 65211, U.S.A.

Abstract

Akrochordite, $(Mn,Mg)_5(OH)_4(H_2O)_4(AsO_4)_2$, monoclinic holosymmetric, $a = 5.682(2)$, $b = 17.627(5)$, $c = 6.832(1)$ Å, $\beta = 99.49(2)°$, $Z = 2$, space group $P2_1/c$, $D_{obs} = 3.19$, 3.26, $D_{calc} = 3.26$ g·cm^{-3} for $(Mn_{0.80}Mg_{0.20})$, has 12 non-H atoms in the asymmetric unit. $R = 0.036$ for 1295 independent F_o. Average distances are $^{[6]}$Mn(1)–O 2.174, $^{[6]}$Mn(2)–O 2.232, $^{[6]}$Mn(3)–O 2.188, and $^{[4]}$As–O 1.686 Å. Bond-distance averages suggest that Mg^{2+} substitutes for Mn^{2+}, with a preference for the Mn(1) site followed by the Mn(3) site.

The perfect {010} cleavage results from a sheetlike structure with formula-unit composition $^{2}_{\infty}[M_5(OH)_4(H_2O)_4(AsO_4)_2]$ parallel to this plane. Of the six unique hydrogen bonds O–H···O, four penetrate the *c*-axial glide planes at $y = 1/4$, $3/4$ and bond symmetry-equivalent sheets together. Two of these bonds involve OW(2) → O(3) 2.79 and OH(6) → OW(2) 3.02 Å, the arrows pointing to hydrogen-bond acceptors and the distances corresponding to oxygen-oxygen separations.

Upon projection along [01$\bar{2}$], it is seen that the sheets are made of fundamental building blocks based on $^{1}_{\infty}[M_5\phi'_2\phi_{12}]$ octahedral walls of amphibole type. In amphiboles, the $\phi' = (OH^-,F^-)$, but in akrochordite it is apical O(1) of the $[AsO_4]$ tetrahedron. These walls are connected in stepwise fashion by O(2) and O(3) of $[AsO_4]$ to form the sheetlike modular units.

The remaining O(4) of $[AsO_4]$ receives three hydrogen bonds, two of which penetrate the *c*-axial glide planes. These have oxygen-oxygen separations OW(1)$^{(2)}$ → O(4) 2.59 and OW(2) → O(4) 2.62 Å. The remaining bond, within the modular unit, is OW(1) → O(4) 2.62 Å. Several examples of oxide terminal to a tetrahedral anionic group are known and include seamanite, metavauxite, and minyulite, all of which possess similar relatively short O–H···O oxygen-oxygen distances, ranging from 2.58 to 2.80 Å.

Introduction

Determining the relationship between crystal structure and phase paragenesis is a prime motivation for any systematic analysis of mineral-chemical crystallography, and members of the $Mn^{2+}_n(OH)^{-}_{2n-3z}(H_2O)_q(AsO_4)^{3-}_z$ series are no exception (Moore and Molin-Case, 1971). The species, although rather exotic, occur in relatively close association with each other, and parageneses were early studied by Sjögren (1885). However, experimentally controlled conditions of temperature, pressure, pH, Eh, etc. are largely unexplored. It is unfortunately too early to reliably apply mineral structures *directly* to mineral paragenesis, and the feasibility of such a relationship is uncertain. One major problem is the lack of any strategy to obtain reliable thermochemical parameters directly from a crystal structure; another is the difficulty in obtaining good temperatures for the growth of successive crystallizing phases.

Akrochordite's name comes from the Greek *akrochordon,* meaning "a wart." And like a wart, its structure solution remained enigmatic. Single crystals, extremely rare, are usually splayed or tapered. Although approximate cell dimensions and space group could be obtained, the crystals were hardly suitable for structure analysis. Interest was attached to akrochordite because it usually crystallizes latest in the sequence of other arsenates.

Experimental details

Several radial aggregates of sharp akrochordite crystals were repeatedly broken until a crystal that yielded reasonable single-crystal precession photographs was obtained. The fragments came from the type specimen of eveite, NRMS 390274, in the Swedish Natural History Museum, which was also used in the original study of Moore (1967). The present unit-cell parameters in Table 1 are in fair agreement with the earlier study. The details of the experimental part of this investigation are summarized in Table 1.

0003–004X/89/0102–0256$02.00

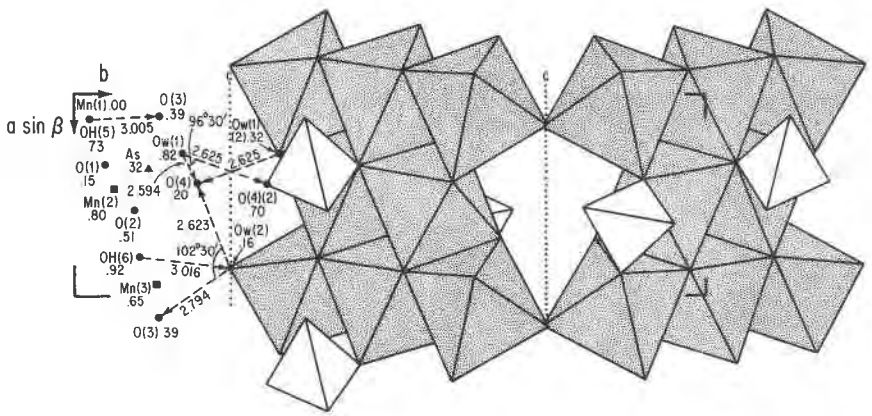

Fig. 1. Polyhedral representation of akrochordite crystal structure along [001]. The asymmetric unit is indicated on the left. Heights are given as fractional units. Hydrogen bond distances, angles, and arrows are included. Note the dotted *c*-glide plane.

Conventional Lorentz, polarization, and absorption corrections were applied by empirical ψ-scan, and scaled transmission coefficients ranged from 0.80–1.00. Solution of the crystal structure was straightforward by means of the MULTAN direct methods procedure (Main et al., 1977). The effect of anomalous dispersion of Mo radiation by Mn, As, and O was included in F_o by using $\Delta f'$ and $\Delta f''$ (Ibers and Hamilton, 1974). All atoms, except H atoms, were located in the asymmetric unit. The initial heavy Mn and As afforded sufficiently precise phase angles so that all remaining oxygen atoms in the asymmetric unit could be located. Refinement was concluded after five cycles of atomic coordinate parameters and anisotropic thermal-vibration parameters showed no significant shifts. It was hoped that H-atom centroids could be located by difference synthesis, but background noise was prominent—a typical observation on crystals with elements beyond the third row. Therefore, hydrogen bonds were inferred by inspection of bond lengths and bond strengths. However, of the six unique H-atom centroids, five appeared among the maxima in difference synthesis, but they were not refined.

Least-squares refinements employed the full-matrix program SHELX-76. The conventional discrepancy indices are listed in Table 1. A total of 108 variable parameters and 1295 independent reflections used in refinement gives a reflection : variable parameter ratio of 12:1. The observed and calculated structure factors are available on request.[1]

Description of the structure

Conventional choices of axial projections disguise the fact that akrochordite is constructed of sheets with formula-unit composition $[M_5^{2+}(OH)_4(H_2O)_4(AsO_4)_2]$, where M^{2+} = principal Mn^{2+} and subordinate Mg^{2+}. Furthermore, these sheets are locally based on cubic close-packed strips of oxygen atoms and are knit to neighboring symmetry-equivalent sheets through four independent, rather strong hydrogen bonds and the [O(1)]–As–[O(2),O(3)] bridge of the arsenate tetrahedron.

A conventional polyhedral diagram projected down the [001] axis is presented in Figure 1. The asymmetric unit consists of labeled atoms in Table 2. The proposed O–H···O hydrogen bonding scheme is shown by dashed arrows in the first quadrant along *b* in the diagram. The *c*-axial glides are also sketched in, and only the hydrogen bonds penetrate these glides. OW(2), which is close to the glide plane, is coordinated by Mn(3) and 3H. Thus, a sheet of formula unit of structure occurs parallel to {010}. The sheet is bounded at $-\frac{1}{4} < y < \frac{1}{4}$ by the *c*-axial glides and only hydrogen bonds penetrate the

Table 1. Experimental details for akrochordite

(A) Crystal cell data	
a (Å)	5.682(2)
b (Å)	17.627(5)
c (Å)	6.832(1)
β (°)	99.49(2)
Space group	$P2_1/c$
Z	2
Formula	$(Mn,Mg)_5(OH)_4(H_2O)_4(AsO_4)_2$
D_x	3.194 (Flink, 1922), 3.26 (Moore, 1967)
D_c (g·cm^{-3})	3.41 (for $Mn_{1.00}$), 3.26 (for $Mn_{0.80}Mg_{0.20}$)
μ (cm^{-1})	91.0 for $Mn_{0.80}Mg_{0.20}$
(B) Intensity measurements	
Crystal size (μm)	150 × 230 × 320
Diffractometer	Enraf-Nonius CAD-4
Monochromator	Graphite
Max (sin θ/λ)	0.65
Scan type	θ-2θ
Maximum scan time (s)	120
Scan width (°)	$\theta = (A + B \tan \theta)$ where $A = 0.9$, $B = 0.35$
Background counts	4/6 time on peak scan, 1/6 time on each side
Radiation	MoK_α (λ = 0.71069 Å)
Measured intensities	1545
Independent F_o	1295, $F_o > 4\sigma$ (F_o) used in refinement
Orientation monitor	After every 200 reflections, 25 reflections used for cell refinement
Intensity monitor	Every 7200 s of X-ray exposure
(C) Refinement of structure	
R 0.036	$R = \Sigma(\|\|F_o\| - \|F_c\|\|)/\Sigma F_o$
R_w 0.037	$R_w = [\Sigma w(\|F_o\| - \|F_c\|)^2/\Sigma w F_o^2]^{1/2}$, $w = \sigma^{-2}(F)$
Weights	Each structure-factor assigned weight $w_F = \sigma^{-2}$
Scattering factors	Neutral Mn, As, and O (Ibers and Hamilton, 1974)

[1] A copy of the observed and calculated structure factors may be ordered as Document AM-89-395 from the Business Office, Mineralogical Society of America, 1625 I Street, N.W., Suite 414, Washington, D.C. 20006, U.S.A. Please remit $5.00 in advance for the microfiche.

Table 2. Akrochordite: Atomic coordinate and anisotropic thermal-vibration parameters (× 10^4)

Atom	x	y	z	U_{11}	U_{22}	U_{33}	U_{23}	U_{13}	U_{12}	B_{eq} (Å²)
M(1)	0	0	0	163(8)	195(8)	150(8)	64(6)	−30(6)	−3(6)	1.34(6)
M(2)	0.4758(2)	0.0618(1)	0.7967(2)	120(5)	144(5)	171(5)	43(4)	−36(4)	6(4)	1.15(4)
M(3)	−0.0566(2)	0.1315(1)	0.6470(2)	159(5)	163(5)	99(5)	15(4)	−16(4)	8(4)	1.11(4)
As	0.3683(1)	0.1185(1)	0.3188(1)	118(3)	102(3)	49(3)	4(2)	−37(2)	2(3)	0.89(2)
O(1)	0.3512(9)	0.0470(3)	0.1483(7)	168(24)	106(23)	116(23)	−32(19)	−63(18)	−1(20)	1.03(18)
O(2)	0.5791(9)	0.0965(3)	0.5149(7)	142(23)	211(26)	86(22)	54(20)	−70(18)	5(21)	1.16(19)
O(3)	0.1033(10)	0.1335(3)	0.3884(7)	233(27)	254(29)	91(23)	19(21)	34(20)	37(23)	1.52(19)
O(4)	0.4380(9)	0.1973(3)	0.2037(7)	218(26)	101(23)	112(23)	−3(19)	13(19)	−22(20)	1.13(19)
OH(5)	0.1252(9)	0.0235(3)	0.7272(7)	182(24)	115(22)	62(21)	−10(18)	−12(18)	9(20)	0.95(18)
OH(6)	0.8144(8)	0.1036(3)	0.9175(7)	153(23)	131(24)	56(20)	2(18)	−22(17)	1(19)	0.89(18)
OW(1)	0.2964(9)	0.1734(3)	0.8232(7)	185(25)	128(24)	84(22)	−9(18)	−37(18)	−28(20)	1.05(19)
OW(2)	0.8588((9)	0.2483(3)	0.1566(8)	176(25)	163(25)	174(25)	6(21)	−34(20)	−7(21)	1.35(20)

Note: The U_{ij} are coefficients in the expression $\exp[-(U_{11}h^2 + U_{22}k^2 + U_{33}l^2 + 2U_{12}hk + 2U_{13}hl + 2U_{23}kl)]$. The equivalent isotropic thermal parameter is $B_{eq} = (8/3)\pi^2(U_{11} + U_{22} + U_{33})$.

boundary along [010]. We propose three unique hydrogen bonds to the O(4) acceptor, which are shown in Figure 1: OW(1)···O(4) 2.59, OW(2)···O(4) 2.62, and OW(1)$^{(2)}$··· O(4) 2.62 Å. In addition, since O(4) also bonds to As, it is undersaturated with electrostatic bond-strength sum $p_0 = \frac{5}{4} + \frac{1}{6} + \frac{1}{6} + \frac{1}{6} = \frac{21}{12} = 1.75$. To evaluate the electrostatic bond-strength sum p_0, we have used bond strengths $s = \frac{5}{6}$ valence units for the hydrogen-bond donor (the hydrogen written H_d) and $s = \frac{1}{6}$ v.u. for the hydrogen-bond acceptor (the hydrogen written H_a) (see Baur, 1970, especially p. 152). As a rather undersaturated anion, all bonds to it are comparatively short.

Baur noted that O–H···O distances between oxygens range from 2.5 to 3.3 Å based on 392 independent data. Note that these distances are between donor and acceptor oxygens. It is clear from three short OW···O(4) distances and one short As–O(4) distance that O(4) is O^{2-} and that the arsenate group is $[AsO_4]^{3-}$ and not $[AsO_3OH]^{2-}$. This is reminiscent of the four possible OH···O(8) bonds determined for seamanite, $Mn_3^{2+}(OH)_2[B(OH)_4][PO_4]$, by Moore and Ghose (1971). Three distances are 2OH(5) ···O(8) 2.71 and OH(4)···O(8) 2.73 Å, and a longer OH(2)···O(8) 2.94 Å also occurs. The P–O(8) 1.517 Å individual distance is shorter than the phosphate tetrahedral average, 1.534 Å, in the structure. Unlike akrochordite, seamanite (R = 0.062) does not possess sheetlike units of crystal structure which are bridged by only hydrogen bonds but rather is a three-dimensional array of ···M–ϕ–T··· bonds. More like akrochordite is metavauxite (R = 0.097), which is $[Fe(H_2O)_6]^{2+}[Al_2(OH)_2(H_2O)_2(PO_4)_2]^{2-}$ (Baur and Rama Rao, 1967), in that it has insular octahedra alternating with octahedral-tetrahedral sheets separated by the {100} plane. The plane is penetrated by three different hydrogen bonds that are accepted by O(4) of the terminal $[PO_4]$ tetrahedron of the sheets: OW(7)···O(4) 2.58,OW(7′)··· O(4) 2.64, and OW(8)···O(4) 2.67 Å. The remaining P–O(4) distance is about the same as the polyhedral average. Another example is O(4) in minyulite, $K[Al_2F(H_2O)_4(PO_4)_2]$ (R = 0.022) which receives four hydrogen bonds (Kampf, 1977). The pertinent distances are OW(2)···O(4) 2.70, OW(1)···O(4) 2.74, OW(2)′···O(4) 2.80, and OW(1)′···O(4) 2.80 Å. Here, the remaining P–O(4) 1.531 distance in minyulite matches within error the polyhedral average, ⟨P–O⟩ 1.532 Å. These four compounds all seem to involve one terminal P–O where that oxide achieves approximate electrostatic neutrality by coordination with three or more hydrogen-acceptor bonds.

Quite different are P–O distances in compounds that appear to have P–O–H··· termini. Termination means no continued bonding to cations other than H from the donor oxygens. In these compounds, the P–O–H··· terminal distances are considerably *longer* (1.57–1.59 Å) than P–O···nH (n = 1–4) terminal distances (1.51–1.55 Å). The shortest distance is for the extremely undersaturated P–O 1.48 Å in anhydrous compounds. This is immediately understandable in terms of local electrostatic neutrality: for P–O–H···, $p_0 = \frac{5}{4} + \frac{5}{6} = \frac{25}{12}$ and for P–O, $p_0 = \frac{15}{12}$—oversaturated and very undersaturated oxides, respectively. Usually, OH^- is an acceptor of at most one hydrogen bond to the oxygen. The terminal O^{2-}, on the other hand, receives three to four hydrogen bonds in hydrated crystals. For this reason, discrimination between the two is usually not difficult. We prefer to designate compounds with at least one P–OH as *acid* phosphates, and those with P–O and no OH^- attachments as *normal* phosphates. The same holds for arsenate; As is in the same Group 5A as P. The *oxo*-terminus in the normal compounds appears to accept several short hydrogen bonds.

In hureaulite, $Mn_5^{2+}(H_2O)_4[PO_3OH]_2[PO_4]_2$ (R = 0.058), the hydroxyl oxygen is bonded to P(1) + H_d (Moore and Araki, 1973). It does not appear to accept hydrogen bonds. The P(1)–OH 1.57 Å distance is longer than its $[PO_3OH]$polyhedral average of 1.54 Å. The synthetic $NH_4Fe_3^{3+}(H_2O)_3[PO_3(OH)_{\frac{1}{3}}O_{\frac{1}{3}}]_3[PO_2(OH)_2]_3 \cdot 3H_2O$ (R = 0.042), structurally investigated by Moore and Araki (1979), was crystallized from distinctly acid solutions with initial pH = 0.5–2.5, final pH = 2 for liquid coexisting with crystals. The acidities were noted in Haseman et al. (1951). The structure has three unique P–OH bonds: P(1)–OH(3) 1.58, P(2)–OH(6) 1.57 and P(2)–OH(8) 1.58 Å, all

longer than the P(1,2)–O 1.54 Å polyhedral average. The OH(3), OH(6), and OH(8) oxygens not only donate but also receive one hydrogen bond each and consequently their oxide fraction is considerably oversaturated. MacGillavry and Rieck (1962) listed the following ranges of bond lengths (in angstroms) for different types of phosphates: P–O = 1.512–1.549 (five determinations) for normal PO_4, P–O = 1.54 (two determinations) and P–OH = 1.58 (two determinations) for the two types of acid phosphates, whereas for "polyphosphates," terminal P–O–P = 1.43–1.52 (seven determinations) and bridging P–O–P = 1.56–1.68 (nine determinations). The normal PO_4 and the acid phosphates already have been discussed. For polyphosphates, the marked difference between terminal and bridging P–O distances can be understood through general undersaturation and oversaturation, respectively, of electrostatic bond-strength sums, p_0, from 2.00.

It was initially believed that normal P–O receiving several hydrogen bonds was paragenetically distinct from acid P–OH in that the former formed only in basic fluids and the latter formed in distinctly acid fluids. If such a relation held, then a neat interpretation could be made between structure and paragenesis. Unfortunately, such a simple explanation is not the key to discriminating between these two bonding types. Haseman et al. (1951) stated that the final pH = 2.8 in minyulite formation, a distinctly acid environment where a terminal P–O receives four hydrogen bonds. Therefore, we prefer the term *normal* phosphate, as distinct from *basic* or *acid* phosphates. Nor is it at all clear whether hureaulite forms under distinctly acid, neutral or basic conditions. In fact, Haseman et al. presented several examples where such phases are evidently stable over a rather wide pH range.

Figure 1 and Table 3 outline the six unique O–H···O bonds in the akrochordite structure. The asymmetric unit and the hydrogen-bond arrows with the heads pointing toward the oxygen acceptor appear in the left quadrant. Two bonds OH(5) → O(3) 3.00 and OW(1) → O(4) 2.59 Å are confined within one sheet, a unit formula shown here bounded by the c-axial glide planes between $y = \frac{1}{4}$ and $y = \frac{3}{4}$. The remaining four unique hydrogen bonds penetrate the c-axial glide plane and hold adjacent sheets together. Included are OW(2) → O(3) 2.79, OH(6) → OW(2) 3.02, OW(1)$^{(2)}$ → O(4) 2.59, and OW(2) → O(4) 2.62 Å. All bonds with O(4) as a receptor have already been discussed, and these are the shortest hydrogen bonds in the structure. The good to perfect {010} cleavage has a simple explanation: only O–H···O bonds are broken. As suggested by this figure, it would be desirable to project a slab of the formula unit normal to the plane of its layer. Projection of akrochordite's structure down x^* reveals the structural principle in Figure 2. Individual fundamental building blocks (fbb) are joined to each other in a staggered fashion. In this diagram, only Mn(1), Mn(2), Mn(3), and As are presented. Lines connect cations that share an oxygen. Hydrogen bonds are ignored. Inversion centers and c-axial glides are shown. Here, a cell transformation is required (100/01$\bar{2}$/012). The new cell, a, b' = [01$\bar{2}$], c' = [012] has $a = 5.682$, $b' = 22.303$, $c' = 22.303$ Å, $\alpha' = 75°34'$, $\beta' = 95°48'$, $\gamma' = 84°12'$ and contains four conventional cells of akrochordite. This cell not only presents the {010} cleavage plane, but it shows the sheet module parallel to {010}. In addition, the fbb can be easily extracted.

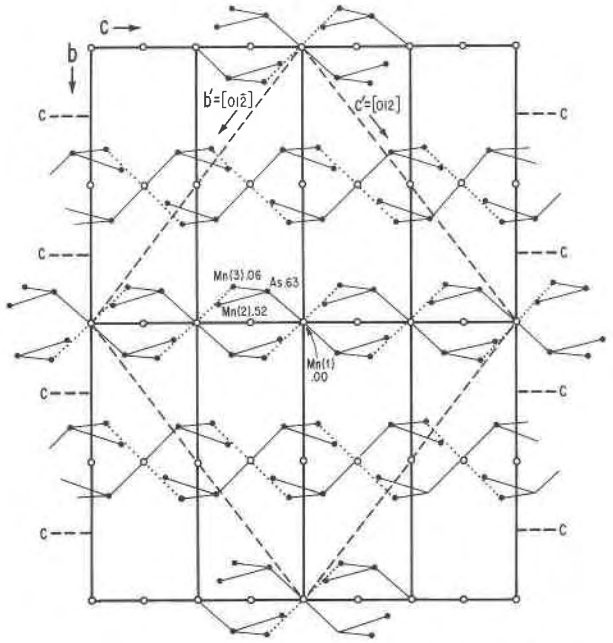

Fig. 2. The Mn and As cations along x^*. The c-glides and inversion centers are shown. Thin lines indicate cation connections via ligands, which are omitted. The central octahedral wall is dotted, and the transformed $b' \times c'$ cell is dashed. Note suggestion of good {010} cleavage.

Dotted lines within the packets of structure indicate the Mn(1), Mn(2), and Mn(3) octahedral edge-sharing wall that runs parallel to the a axis. This wall is like the octahedral wall found in amphiboles. All oxygens except O(4), which is coordinated by As and 3H, are components of the wall. Note that the sequence of five Mn(1), Mn(2), and Mn(3) cations projected down x^* progresses Mn(3) ($x \approx 0$), Mn(2) ($x \approx \frac{1}{2}$), Mn (1) ($x \approx 0$), Mn(2)' ($x \approx \frac{1}{2}$), Mn(3)' ($x \approx 0$), and that b' and c' are alternately roughly perpendicular and parallel to these walls. Projection along b' = [01$\bar{2}$] should afford a slab roughly normal to that axis, from which the packing principle can be ascertained. Along b', the $M_5\phi_{14}$ wall is nearly normal to that axis at $y' = \frac{1}{8}, \frac{3}{8}, \frac{5}{8}, \frac{7}{8}$ and nearly parallel to that axis at $y' = \frac{0}{8}, \frac{2}{8}, \frac{4}{8}, \frac{6}{8}$. Figure 3 shows that wall at $y' \approx \frac{7}{8}$ with Mn(1) fixed at ($\bar{x}\bar{y}\bar{z}$) = (0 $\frac{7}{8}$ $\frac{5}{8}$). The arrangement of the wall is based on a slice of cubic close-packing [ABCA]. Each wall has stoichiometry $M_5(OH)_4(H_2O)_4(AsO_4)_2$; thus all atoms in the asymmetric unit are represented, and this unit is chosen as the fbb of the structure. The $[AsO_4]$ tetrahedra decorate the central $^1_\infty[M_5\phi_{14}]$ octahedral edge-sharing wall by sharing the apical O(1) vertex above and below the projection, and the O(2) and

TABLE 3. Akrochordite: Polyhedral interatomic distances (Å) and angles (°)

M(1)			**M(3)**		
2 M(1)–OH(6)	2.137		M(3)–O(3)	2.116	
2 M(1)–OH(5)	2.142		M(3)–OH(6)	2.155	
2 M(1)–O(1)	2.242		M(3)–OW(2)‡	2.176	
Average	2.174		M(3)–OH(5)	2.192	
		O–Me–O′	M(3)–O(2)	2.206	
2 OH(5)–OH(6)*	2.749	79.9	M(3)–OW(1)	2.285	
2 O(1)–OH(6)*†	2.827	80.4	Average	2.188	
2 O(1)–OH(5)*	2.980	85.6	OH(5)–OH(6)*	2.749	78.4
2 O(1)–OH(5)†	3.218	94.4	OH(5)–OW(1)*	2.853	79.2
2 OH(5)–OH(6)†	3.280	100.1	O(2)–OH((6)*	2.856	81.8
2 O(1)–OH(6)	3.346	99.6	OW(1)–OW(2)‡	2.908	81.3
Average	3.067	90.0	O(3)–OW(1)	3.074	88.5
M(2)			O(3)–OH(5)	3.103	92.2
M(2)–OH(5)	2.083		OH(6)–OW(1)	3.164	90.9
M(2)–OH(6)	2.098		OH(6)–OW(2)‡	3.195	95.1
M(2)–O(1)†	2.159		O(2)–OW(2)‡	3.231	95.0
M(2)–O(2)	2.191		O(3)–OW(2)‡	3.236	97.9
M(2)–OW(1)	2.237		O(2)–O(3)	3.300	99.5
M(2)–O(1)	2.627		O(2)–OH(5)	3.310	97.6
Average	2.232		Average	3.082	89.8
O(1)†–OH(6)*	2.827	83.2	**As**		
OH(5)–OW(1)*	2.853	82.6	As–O(3)	1.673	
O(2)–OH(6)*	2.856	83.5	As–O(4)	1.674	
O(1)–OH(5)	2.980	77.6	As–O(2)	1.688	
O(1)–OW(1)	3.125	79.5	As–O(1)	1.709	
O(2)–OW(1)	3.157	90.9	Average	1.686	
OH(6)–OW(1)	3.164	93.7	O(3)–O(4)	2.695	107.3
O(1)†–OH(5)	3.218	98.7	O(1)–O(4)	2.709	106.4
O(1)–O(1)*†	3.292	86.3	O(1)–O(2)	2.765	109.0
O(2)–OH(5)	3.310	101.5	O(2)–O(3)	2.776	111.4
O(1)†–O(2)	3.399	102.8	O(2)–O(4)	2.785	111.9
O(1)–OH(6)	3.432	92.5	O(1)–O(3)	2.786	110.9
Average	3.134	89.4	Average	2.753	109.5
	Hydrogen bonds				
OW(1)‡	→O(4)	2.594			
OW(2)	→O(4)	2.623			
OW(1)	→O(4)	2.625			
Average		2.614			
OW(2)	→O(3)	2.794			
OH(5)	→O(3)	3.005			
OH(6)	→OW(2)	3.016			

Note: Under each atom heading are listed bond distances and angles. The errors are M–O, As–O < 0.005 Å, O–O′ < 0.008 Å.
* Shared edges between polyhedra, all associated with M.
† Equivalent points (referred to Table 2): $-x, -y, -z$.
‡ Equivalent points (referred to Table 2): $x, \frac{1}{2} - y, \frac{1}{2} + z$.

O(3) vertices at the boundary of the wall. This projection clearly shows the similarity of the octahedral wall to the corresponding portion of the amphibole structure. The $^{1}_{\infty}[M_5\phi_{14}]$ wall of amphibole type can be written $^{1}_{\infty}[M_5\phi'_2\phi_{12}]$, where the $\phi' = (OH^-,F^-)$ corresponds to the central anion on the mirror plane of the $C2/m$ clinoamphiboles that divides the wall into two halves. In akrochordite, this position corresponds to the apical O(1) of the $[AsO_4]$ tet-

TABLE 4. Akrochordite: Pauling electrostatic valence balance of cations and anions

	Cations						
Anions	M(1)	M(2)	M(3)	As	H_d	H_a	p_0
O(1)	+0.07	**−0.07**, +0.40	—	+0.02	—	—	2.25
O(2)	—	−0.04	**+0.02**	**+0.00**	—	—	1.92
O(3)	—	—	−0.07	−0.01	—	2 × ⅙	1.92
O(4)	—	—	—	−0.01	—	3 × ⅙	1.75
OH(5)	−0.03	−0.15	**+0.00**	—	⅚	—	1.83
OH(6)	−0.04	−0.13	−0.03	—	⅚	—	1.83
OW(1)	—	+0.01	+0.10	—	2 × ⅚	—	2.33
OW(2)	—	—	**−0.01**	—	2 × ⅚	⅙	2.17

Note: Bond length–bond strength contradictions are in **boldface.** The entries are individual deviations from polyhedral averages. Bond strengths for donors (O–H = H_d) and acceptors (O–H···O = H_a) are also listed. Note contradictions give relatively small distance deviations.

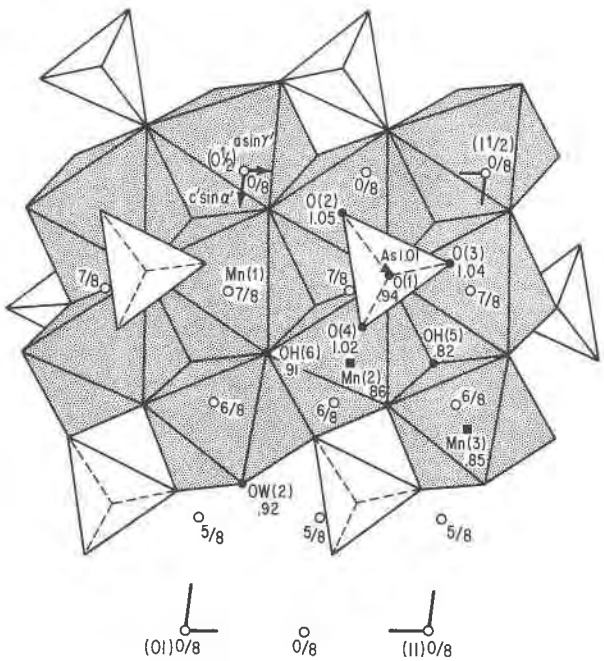

Fig. 3. A wall of polyhedra projected along [01$\bar{2}$] in akrochordite. Note amphibole-like $^{1}_{\infty}[M_3O_{14}]$. Inversion centers are drawn in and derive from Fig. 2.

rahedron (see Fig. 3). Also at the boundary are terminal OW(1) bonded to two octahedra and OW(2) bonded to one octahedron only. The OH(5) and OH(6) complete the coordinating anions and occur between the center and the boundary of the wall. Successive fbb's are linked via O(1), O(2), O(3), and O(4) of the [AsO_4] group. The O(1) is a part of the wall, and O(2) and O(3) link to the boundary vertices of adjacent walls, while O(4) receives three hydrogen bonds.

The two orientations of these walls are automatically defined by the inversion centers and the *c*-axial glide implicit in $P2_1/c$ (Fig. 2). The packing efficiency or volume per oxygen atom is V_E = 21.1 Å^3, similar to other basic manganous arsenates with strips of dense-packing and close to manganosite (4MnO), V_E = 21.9 Å^3, which has the rock-salt structure.

The octahedral wall along [100] and nearly perpendicular to [01$\bar{2}$] shares with most of the other basic manganous arsenates strips or fragments of the pyrochroite, $Mn^{2+}(OH)_2$, sheet. A *wall* is intermediate between a chain, which is parallel to some axis, and a sheet, which is parallel to some plane. In other words, a wall is a chain with finite thickness. Or it can be considered a strip or a section of a sheet. For an octahedral wall, thickness can be specified by the number of octahedra, followed sequentially until the motif is repeated. In Figure 3, it is seen that the wall in the {012} plane runs parallel to the [100] direction and the thickness is parallel to [001]′. In thickness, two octahedra alternate with three octahedra sequentially, or (·23·). Included are octahedral strips or walls in retzian (·11· strip), arsenoklasite (·12· wall), allactite (·22· wall), akrochordite (·23· wall), chlorophoenicite (·33· wall), and several others with fragments that further link to form edge- and corner-sharing frameworks. What controls the extent of polymerization of the fragments, strips, walls, etc., why most are based on close-packing, and what is the connection between structure and paragenesis in these interesting compounds are as yet unanswered questions.

Table 4 presents electrostatic bond-strength sums, p_0, for the eight unique O anions in akrochordite and the coordinating cations including H_d (s = ⅚), H_a (s = ⅙), M(1), M(2), M(3), and As. Deviations (in Å) from polyhedral averages are listed. Of the 19 independent distance entries, 15 conform with oversaturation ($p_0 > 2.00$) or undersaturation ($p_0 < 2.00$) of the oxide anions by the coordinating cations. This leads to matching for bond length–bond strength deviations in about 80% of the entries, a typical value for oxysalts. The contradictions remaining are small.

Bond distances

Table 3 lists the individual bond distances for our akrochordite. The expected $^{[6]}Mn^{2+}$–$^{[4]}O^{2-}$ 2.20 Å average from Shannon and Prewitt (1969) suggests that Mg^{2+} preferentially substitutes at the Mn(1) site (⟨Mn(1)–O⟩ 2.17), followed by the Mn(3) site (⟨Mn(3)–O⟩ 2.19 Å). Since we applied scattering factors for neutral Mn at the M(1), M(2), and M(3) sites, the thermal-vibration parameters in Table 2 should indicate site preferences. Comparison with thermal-vibration parameters for other refined manganous arsenates indicates that B_{eq} are all somewhat high by about 25%, Mn(1) possessing the largest value. Based on the analysis of Almström in Flink (1922) for type akrochordite, the allocation for 10.0 M in the unit cell indicates a magnesian compound with $7.6Mn^{2+} + 2.4Mg^{2+}$ in the cell. Ordering of Mg is clearly not completely allocated to one site. It is likely that Mg substitutes at M(1) followed by M(3). Note that we have included M(2)–O(1) 2.627 Å into the octahedral coordination sphere. This long distance is common among many of the basic manganous arsenates. The coordination number is difficult to assess. Perhaps the coordination number should be written $^{[5+1]}M(2)$.

For the ten unique shared edges, nine of them are the shortest for their polyhedra. The one exception, O(1)–O(1)$^{(1)}$, is associated with the long M(2)–O(1) distance.

Summary

Akrochordite, $^{2}_{\infty}(Mn,Mg)_5(OH)_4(H_2O)_4(AsO_4)_2$, belongs to the general family of basic manganous arsenate minerals, $Mn^{2+}_n(OH)^{-}_{2n-3z}(H_2O)_q(AsO_4)^{3-}_z$. It is among the latest arsenates to crystallize in a paragenetic sequence.

The underlying unit or fundamental building block is a $^{1}_{\infty}[M_5\phi_{14}]$ wall of octahedra, resembling the octahedral wall in amphibole. This wall is decorated by the [AsO_4] tetrahedron, which shares the central O(1) vertex (the OH, F position of amphibole), and the O(2) and O(3) of symmetry-equivalent tetrahedra at the boundary of the wall.

The $[AsO_4]$ tetrahedron thus creates a steplike sequence of equivalent walls to form a sheetlike arrangement of polyhedra parallel to {010}, the plane of perfect cleavage.

Six independent O–H···O bonds occur in the structure. Two of these bonds are confined within a sheet, and four penetrate the *c*-axial glide planes at $y = \frac{1}{4}$ and $\frac{3}{4}$. The anion O(4) is four-coordinated: in addition to receiving the As^{5+} ($s = \frac{5}{4}$ v.u.) bond, it receives three short (2.59–2.62 Å) hydrogen ($s = \frac{1}{6}$ v.u. each) bonds. It shares this property in common with several other mineral structures such as seamanite, metavauxite, and minyulite.

The common underlying structural feature among basic manganous arsenates appears to be walls of octahedra that in turn are fragments of the pyrochroite, $Mn(OH)_2$ structure. What environments dictate thicknesses and close-packings of walls, and the connection between their structures and paragenesis, remain as yet unanswered questions.

Acknowledgments

P.B.M. appreciates support by the National Science Foundation (Grant EAR-84-08164), and P.K.S. thanks the Tennessee computation facilities at the Tennessee Earthquake Information Center for use of their VAX computer.

References cited

Baur, W.H. (1970) Bond length variation and distorted coordination polyhedra in inorganic crystals. Transactions of the American Crystallographic Association, 6, 129–155.

Baur, W.H., and Rama Rao, B. (1967) The crystal structure of metavauxite. Die Naturwissenschaften, 21, 1–2.

Flink, G. (1922) Akrochordit, ett nytt mineral från Långbans gruvor. Geologiska Föreningen i Stockholm Förhandlingar, 44, 773–776.

Haseman, J.F., Lehr, J.R., and Smith, J.P. (1951) Mineralogical character of some iron and aluminum phosphates containing potassium and ammonium. Soil Science Society of America Proceedings 150, 15, 76–84.

Ibers, J.A., and Hamilton, W.C., Eds. (1974) International tables for X-ray crystallography, vol. 4. p. 149. Kynoch Press, Birmingham, England.

Kampf, A.R. (1977) Minyulite: Its atomic arrangement. American Mineralogist, 62, 256–262.

MacGillavry, C.H., and Rieck, G.D., Eds. (1962) International tables for x-ray crystallography, vol. 3. p. 258. Kynoch Press, Birmingham, England.

Main, P., Woolfson, M.M., Lessinger, L., Germain, S., and Declerq, J.P. (1977) MULTAN 74, a system of computer programs for the automatic solution of crystal structures. University of York, England.

Moore, P.B. (1967) Contributions to Swedish mineralogy. Studies on the basic arsenates of manganese: Retzian, hemafibrite, synadelphite, arsenoclasite, arseniopleite, and akrochordite. Arkiv för Mineralogi och Geologi, 4, 425–443.

Moore, P.B., and Araki, T. (1973) Hureaulite, $Mn_5^{2+}(H_2O)_4[PO_3(OH)]_2[PO_4]_2$: Its atomic arrangement. American Mineralogist, 58, 302–307.

——— (1979) Crystal structure of synthetic $(NH_4)H_8Fe_3^{3+}(PO_4)_6 \cdot 6H_2O$. American Mineralogist, 64, 587–592.

Moore, P.B., and Ghose, S. (1971) A novel face-sharing octahedral trimer in the crystal structure of seamanite. American Mineralogist, 56, 1527–1538.

Moore, P.B., and Molin-Case, J. (1971) Crystal chemistry of the basic manganese arsenates: V. Mixed manganese coordination in the atomic arrangement of arsenoclasite. American Mineralogist, 56, 1539–1552.

Shannon, R.D., and Prewitt, C.T. (1969) Effective ionic radii in oxides and fluorides. Acta Crystallographica, B25, 925–946.

Sjögren, Hj. (1885) IX. Ueber die Manganarseniate von Nordmarken in Wermland. Zeitschrift für Krystallographie, 10, 113–155.

Manuscript received December 14, 1987
Manuscript accepted September 30, 1988